JASA ARTICLE

Sound power determination by intensity—Are field indicators and criteria in ISO 9614 meaningful?

Volker Wittstock,[1,a)] Spyros Brezas,[2] and Fabian Heisterkamp[3]
[1]Physikalisch-Technische Bundesanstalt, Braunschweig 38118, Germany
[2]Department of Music Technology and Acoustics, Hellenic Mediterranean University E. Daskalaki, Perivolia, 74133 Rethymno, Greece
[3]Federal Institute for Occupational Safety and Health (BAuA), Friedrich-Henkel-Weg 1-25, 44149 Dortmund, Germany

ABSTRACT:
The three parts of ISO 9614 describe methods for the determination of the sound power level of noise sources. According to these standards, measured sound power levels must be qualified by comparing several sound field indicators to given criteria. This procedure is investigated by analytical calculations with monopole and dipole sources. Their sound fields are superposed with extraneous free and diffuse sound fields. When the ISO 9614 method is applied to these cases, it turns out that the signed pressure intensity indicator is well suited to qualify the measured sound power level. In contrast to this, the unsigned pressure intensity indicator and the field non-uniformity indicator fail to describe the quality of the determined sound power level. This theoretical finding is verified by a large measurement program.
https://doi.org/10.1121/10.0024361
(Received 8 September 2023; revised 4 December 2023; accepted 15 December 2023; published online 23 January 2024)
[Editor: William James Murphy] Pages: 588–599

I. INTRODUCTION

The sound power level (SWL) L_W is the key quantity to describe the noise emissions of products, machines, and equipment. For example, the following regulations use the SWL to describe the noise emission of some or all of the products in their scope: the European Outdoor Noise Directive,[1] the Australian approach to noise labelling,[2,3] the European Machinery Directive,[4] and the EU energy label for certain products in the scope of the European Ecodesign Directive.[5,6]

Furthermore, the SWL of machines, products, and equipment is the input quantity for the prediction of sound pressure levels[7,8] in workshops and other rooms, where these products are operated. This prediction supports the safe and ergonomic design of factories, workshops, etc. with regard to noise and allows for the evaluation of the effects of room acoustic treatments and other noise control measures before they are implemented.

Thus, determining the SWL is important for environmental protection, for occupational health and safety, for product safety, and to inform consumers about the performance of a product regarding its noise emission. Ten different international standards can be used to determine the SWL. They differ on the required measurement equipment and the acoustic environment and yield results with different grades of accuracy.

These standards (see ISO 3740[9] for an overview) can be divided into two main groups: those based on measuring the sound pressure level—the ISO 3740[9] series of standards—and those based on measuring the sound intensity—the ISO 9614 set of standards (Parts 1–3).[10–12] The former rely on cheaper measurement equipment but encounter more restrictions regarding the acoustic environment. Here, the measurements must either be performed in special acoustic environments—hemi-anechoic chambers, reverberation rooms, or outdoors—or be corrected regarding reflections in the room, the so-called environmental correction, and the background noise.

Outside of acoustic test facilities but indoors, one often finds that no measurements with sufficient accuracy, e.g., engineering grade, can be performed or that the conditions do not allow for a measurement that is compliant with the standard at all, e.g., because the environmental correction exceeds the limit in the standard used. In contrast to this, the sound intensity method works well outside of acoustic test facilities, and its application is mainly limited by the level and stationarity of the background noise, if present.

Nevertheless, the methods based on sound pressure measurements are more frequently used. ISO 3744[13] is referred to in the European Outdoor Noise Directive[1] and in many machine-specific noise test codes and safety standards, so-called C-standards in the European standardization jargon.

There are several potential reasons why the sound intensity method is rarely used despite its advantages. The current version of the ISO 9614[10–12] set of standards uses partly inconsistent terminology. The older parts, ISO 9614-1[10] and ISO 9614-2,[11] date to 1993 and 1996, respectively; have not

a)Email: Volker.Wittstock@ptb.de

https://doi.org/10.1121/10.0024361

been revised since; and, apparently, do not correspond to the state-of-the-art. Recent technological and scientific advances have yet to be included in these standards (see also Sec. II). These standards use three major field indicators to assess the quality of the measured SWL. Depending on their values, more measurement points or even a completely new measurement, e.g., on another measurement surface, might be necessary to achieve the desired grade of accuracy. Still, in certain sound field situations, one might have no result regarding the SWL in the end. This approach makes determining the SWL with the sound intensity method quite laborious and complicated.

This paper aims at proposing ways to simplify and improve the sound intensity method. We present results regarding the correlation between the currently used field indicators and the deviation of the measured SWL from the actual SWL. The results hint at the fact that there might be room for simplification of the sound intensity method by using fewer field indicators to assess the quality of the measured SWL.

Section II describes the current knowledge regarding the relation between measured SWLs and the indicator-based standardized criteria for the intensity measurement method. The paper continues with a theoretical investigation of the correlation of the currently used field indicators with the deviation of the measured SWL from the actual SWL in Sec. III. Section IV shows the results of experiments that aim to test whether or not the theoretical results can be confirmed by measurements, while Sec. V presents the conclusions based on Secs. III and IV.

II. INVESTIGATED INDICATORS AND CRITERIA IN ISO 9614

The intensity method for the determination of sound power is an enveloping surface method. This means that the normal component of the sound intensity is measured on a hypothetical surface enveloping the source under test. Sound field indicators are local or surface-averaged quantities that are "intended to help the experimenter in evaluating and interpreting experimental data."[14] In the specific case of ISO 9614,[10–12] they are used in combination with given criteria to assess the measurement conditions to achieve a desired grade of accuracy of the measured SWL. As an intermediate step, modifications of the measurement setup like increasing or decreasing the measurement distance, increasing the number of discrete measurement points, or increasing the scan line density may be necessary. In certain very unfavorable field situations, it is possible that no valid SWL can be obtained according to ISO 9614-1.[10]

With N discrete measurement points on the enveloping surface, the measured sound power P_{meas} is given by

$$P_{\mathrm{meas}} = \sum_{i=1}^{N} I_{\mathrm{meas},i}\, S_i = \sum_{i=1}^{N} \left(I_{\mathrm{n},i} + I_{\mathrm{res},i}\right) S_i, \tag{1}$$

where i indicates the measurement point, S_i the partial surface represented by the ith measurement point, $I_{\mathrm{meas},i}$ the measured sound intensity, $I_{\mathrm{n},i}$ the normal component of the sound intensity, and $I_{\mathrm{res},i}$ the residual sound intensity. Thus, the physically existing normal component of the sound intensity is linearly superposed by the residual intensity, an error contribution resulting from using the two-microphone (p-p) technique. Its level can be calculated from the sound pressure level $L_{p,i}$ at the ith measurement position by[15,16]

$$L_{I,\mathrm{res},i} = L_{p,i} - \delta_{pI0} \tag{2}$$

with the pressure-residual intensity index δ_{pI0}. Here, and in the further course of the paper, it is assumed that the impedance of air is exactly $400\,\mathrm{N\cdot s/m^3}$ and that the reference value for all sound pressure levels is $2\times10^{-5}\,\mathrm{Pa}$, for all intensity levels $10^{-12}\,\mathrm{W/m^2}$ and for all SWLs $10^{-12}\,\mathrm{W}$. The pressure-residual intensity index δ_{pI0} is an instrument-specific quantity, which is measured separately in a sound field with a vanishing pressure gradient, e.g., in a coupler. In such a field, the sound pressure level $L_{p,\Delta p=0}$ and the level of the residual intensity $L_{I,\mathrm{res}}$ are measured. Their difference is a measure for the phase mismatch $\Delta\phi$ between the two measurement channels of the p-p probe, which holds two microphones at a distance $2\,\Delta r$,[16]

$$\delta_{pI0} = L_{p,\Delta p=0} - L_{I,\mathrm{res}} \approx 10\,\lg\left|\frac{k\,2\,\Delta r}{\Delta\phi}\right|\,\mathrm{dB}, \tag{3}$$

where k is the wave number. Combining Eqs. (1) and (2) gives the difference between the level of the measured sound power P_{meas} and the level of the correct sound power P,

$$P = \sum_{i=1}^{N} I_{\mathrm{n},i}\, S_i \tag{4}$$

as[16]

$$\begin{aligned}\Delta L_W &= 10\,\lg\frac{P_{\mathrm{meas}}}{P}\,\mathrm{dB}\\ &= -10\,\lg\left|1-\mathrm{sgn}(\Delta\phi)\,10^{0.1\,(F_{pI\mathrm{n}}-\delta_{pI0})/\mathrm{dB}}\right|\mathrm{dB},\end{aligned} \tag{5}$$

where $\mathrm{sgn}(\Delta\phi)$ describes the sign of the phase mismatch,

$$\mathrm{sgn}(\Delta\phi) = \begin{cases} 1 & \text{when } \Delta\phi \geq 0,\\ -1 & \text{when } \Delta\phi < 0,\end{cases} \tag{6}$$

and

$$F_{pI\mathrm{n}} = \overline{L_p} - \overline{L_{I,\mathrm{meas}}} \tag{7}$$

is the signed pressure intensity indicator. Here, $\overline{L_p}$ is the surface-averaged sound pressure level and $\overline{L_{I,\mathrm{meas}}}$ the surface-averaged level of the measured normal component of the sound intensity, which includes the residual intensity. To limit the measurement deviation due to the phase mismatch, all parts of ISO 9614[10–12] require

$$F_{pI\mathrm{n}} - \delta_{pI0} < -K\,\mathrm{dB}, \tag{8}$$

where K is 10 for precision and engineering grade and 7 for survey grade. According to Eq. (5), this limits $|\Delta L_W|$ to values below 0.5 dB for precision and engineering grade and to values below 1.0 dB for survey grade measurements.

In addition to criterion (8), all parts of ISO 9614[10–12] require, furthermore, that

$$F_{p|I\mathrm{n}|} - F_{pI\mathrm{n}} < 3\,\mathrm{dB} \tag{9}$$

with the unsigned pressure intensity indicator

$$F_{p|I\mathrm{n}|} = \overline{L_p} - \overline{L_{|I,\mathrm{meas}|}}\,. \tag{10}$$

Whereas criterion (8) follows directly from Eq. (5), a clear physical explanation for criterion (9) is, to the knowledge of the authors, not available.

To limit the measurement uncertainty due to imperfect sampling, the field non-uniformity indicator

$$F_\mathrm{S} = \frac{1}{\overline{I_\mathrm{meas}}}\sqrt{\frac{1}{N-1}\sum_{i=1}^{N}\left(I_{\mathrm{meas},i} - \overline{I_\mathrm{meas}}\right)^2} \tag{11}$$

is used. For measurements at discrete positions,[10] the minimum number of measurement positions is

$$N_\mathrm{min} > C F_\mathrm{S}^2, \tag{12}$$

where the factor C is calculated from the assumption of statistically independent samples on the enveloping surface and the given standard deviation of reproducibility of the method.[10] For precision and engineering grade, the standard deviation of reproducibility depends on frequency, and so does the factor C. It is between 11 and 57. For survey grade, only the A-weighted SWL is considered. C is 8 in this case. This criterion has been in discussion for some time (see, e.g., Jacobsen[14] and Hübner[17]). There are further indicators and criteria used in ISO 9614[10–12] that are not examined in this contribution.

III. THEORETICAL INVESTIGATION ON THE USEFULNESS OF SELECTED INDICATORS

A. Basic approach

To investigate the usefulness of the indicators introduced in clause II, field configurations with single monopoles and single dipoles are considered. The sound pressure field created by these sources is superposed by a plane wave and an additional diffuse field, both of varying amplitude. The resulting sound field around the sound sources is sampled at N field points on an enveloping hemisphere or sphere by a p-p probe with an assumed pressure-residual intensity index δ_{pI0}. The field point distribution is chosen so that each point represents the same area. The SWL obtained from this simulated measurement is finally compared to the known SWL of the monopole or dipole as a function of the standardized indicators from clause II.

B. Monopole

1. Theoretical model

The starting point is the sound intensity measured by a probe comprising microphones A and B at a distance $2\,\Delta r$. The probe has a pressure-residual intensity index δ_{pI0}. The sound intensity indicated by the probe is then

$$I_\mathrm{meas} = \frac{|p_\mathrm{A}|\,|p_\mathrm{B}|}{4\,\rho\,c\,k\,\Delta r}\sin\left(\phi_\mathrm{A} - \phi_\mathrm{B}\right) + \frac{\mathrm{sgn}(\Delta\phi)}{8\,\rho\,c}\left(|p_\mathrm{A}| + |p_\mathrm{B}|\right)^2 10^{-0.1\,\delta_{pI0}/\mathrm{dB}}, \tag{13}$$

with the modulus of the sound pressures p at microphones A and B, the impedance of air $\rho\,c$, the phase difference $\phi_\mathrm{A} - \phi_\mathrm{B}$ of the sound pressures at microphones A and B, and the sign of the phase mismatch between the two channels $\mathrm{sgn}(\Delta\phi)$. The sound pressure at microphones A and B is considered to be induced by a monopole with a volume flow q placed at the origin of a spherical coordinate system (r, φ, θ), which is superposed by a plane wave of amplitude a traveling in the positive x-direction (expressed in spherical coordinates as $r\cos\varphi\sin\theta$) and a diffuse sound pressure of amplitude b,

$$p_\mathrm{A/B} = \frac{\mathrm{j}\,\rho\,c\,k\,q\,\mathrm{e}^{-\mathrm{j}\,k\,(r\mp\Delta r)}}{4\,\pi\,(r\mp\Delta r)} + a\,\mathrm{e}^{-\mathrm{j}\,k\,(r\mp\Delta r)\cos\varphi\sin\theta} + b. \tag{14}$$

Here, j is the imaginary unit, and the probe is oriented in such a way that microphone A is closer to the monopole than microphone B. Then the minus sign (−) applies for microphone A, whereas the plus sign (+) does for microphone B. The diffuse field pressure amplitude b measured at field points A and B does not have a phase because the sound pressures at different field points are uncorrelated in an ideal diffuse field and, thus, do not have a distinct phase relation when averaged over time.

Introducing Eq. (14) into Eq. (13) yields the measured intensity. By assuming a negligible correlation between the different sound pressure fields, the time integrals of the products $q\,a$, $q\,b$, and $a\,b$ vanish. Then a relatively simple expression for the related radial component of intensity is achieved,

$$I_\mathrm{r} = \left\{\frac{\sin(k\,2\,\Delta r)}{\left[1 - (\Delta r/r)^2\right]k\,2\,\Delta r} + a_\mathrm{r}^2\,\frac{\sin(k\,2\,\Delta r\cos\varphi\sin\theta)}{k\,2\,\Delta r}\right\} + \mathrm{sgn}(\Delta\phi)\,p_\mathrm{r}^2\,10^{-0.1\,\delta_{pI0}/\mathrm{dB}}, \tag{15}$$

where the measured intensity is related to the area of the enveloping surface S and the sound power of the monopole P_Mon,

$$I_\mathrm{r} = I_\mathrm{meas}\,\frac{S}{P_\mathrm{Mon}}. \tag{16}$$

Furthermore, a related sound pressure is used in Eq. (15),

https://doi.org/10.1121/10.0024361

$$p_\mathrm{r} = \frac{1}{2}\left\{\sqrt{\left[\frac{1}{(1-\Delta r/r)}\right]^2 + a_\mathrm{r}^2 + b_\mathrm{r}^2} + \sqrt{\left[\frac{1}{(1+\Delta r/r)}\right]^2 + a_\mathrm{r}^2 + b_\mathrm{r}^2}\right\}, \tag{17}$$

which is calculated from the related amplitude of the plane wave a_r and the related sound pressure of the diffuse field b_r. They are both related to the sound pressure induced by the monopole by

$$a_\mathrm{r} = a\,\frac{4\pi r}{\rho c k q}; \quad b_\mathrm{r} = b\,\frac{4\pi r}{\rho c k q}. \tag{18}$$

Apart from the finite difference approximation, which is expressed by the geometrically adapted sinc-functions in Eq. (15), the theoretical model does not include any dependency on frequency. Since the finite difference approximation is not in the scope of this contribution, the following calculation results are given for a sufficiently small parameter $k\,2\,\Delta r$.

2. Calculation results for very large numbers of measurement points

Due to symmetry, only the upper hemisphere of a surrounding sphere is discretized by a mesh of 2117 points, which acceptably represent equal areas (Fig. 1). The difference between the measured and the theoretical SWL of the monopole is then obtained by averaging the related intensity from Eq. (15). Surface averaging of the related pressure and of the modulus of the related intensity then enables a calculation of the indicators $F_{pI\mathrm{n}}$ and $F_{p|I\mathrm{n}|}$, whereas the minimum number of discrete measurement points is calculated from Eq. (12) with the indicator F_S from Eq. (11).

To cover a relevant range of the indicators, the sum of the amplitudes of the extraneous sound fields is varied according to

$$\sqrt{a_\mathrm{r}^2 + b_\mathrm{r}^2} = 0.1, \ldots, 100, \tag{19}$$

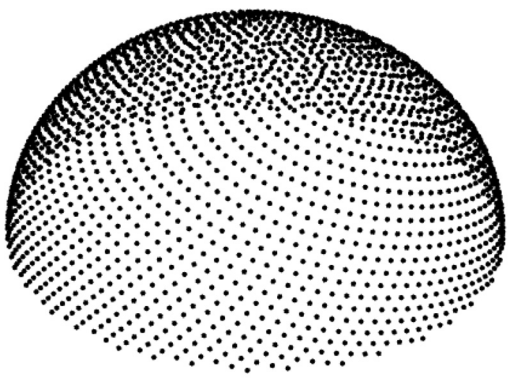

FIG. 1. Upper hemisphere discretized by 2117 points.

and the ratio between the related diffuse field amplitude b_r and the related plane wave amplitude a_r is set to three fixed values,

$$b_\mathrm{r}/\,a_\mathrm{r} = 0.1;\ 1;\ 10, \tag{20}$$

thereby simulating a predominantly direct or diffuse extraneous sound field and an intermediate case.

The SWL difference, i.e., the difference between the measured SWL and the known SWL of the monopole, is a clear function of the pressure intensity criterion $F_{pI\mathrm{n}} - \delta_{pI0}$ (Fig. 2). For very small values of $F_{pI\mathrm{n}} - \delta_{pI0}$, the SWL difference approaches 0 dB, as expected. There are two branches obtained, one for $\mathrm{sgn}(\Delta\phi) = 1$ and one for $\mathrm{sgn}(\Delta\phi) = -1$. The nature of the extraneous sound field does not influence the result at all. Therefore, all three curves are identical. It is furthermore noticeable that these results match excellently the theoretical result from Eq. (5), thereby validating the calculation model. Figure 2 indicates clearly that limiting $F_{pI\mathrm{n}} - \delta_{pI0}$ to certain values is appropriate to limit the SWL difference.

When the SWL difference is plotted as a function of the difference between the unsigned and the signed pressure intensity indicators $F_{p|I\mathrm{n}|} - F_{pI\mathrm{n}}$, different curves are obtained for different sound fields (Fig. 3). Whereas large values of the indicator correlate with large SWL deviations for the predominantly free external field ($b_\mathrm{r}/a_\mathrm{r} = 0.1$) and the mixed extraneous field ($b_\mathrm{r}/a_\mathrm{r} = 1$), the indicator totally fails for the predominantly diffuse field ($b_\mathrm{r}/a_\mathrm{r} = 10$). A limitation of the SWL difference by an application of an upper limit for $F_{p|I\mathrm{n}|} - F_{pI\mathrm{n}}$, thus, requires knowledge of the nature of the sound field.

Similarly, the relation between the SWL difference and the minimum number of measurement points calculated according to Eq. (12) shows significant differences depending on the nature of the extraneous sound field (Fig. 4). The direct calculation result for the minimum number of measurement points is presented here on a logarithmic scale to handle the huge dynamic range. Of course, sound power

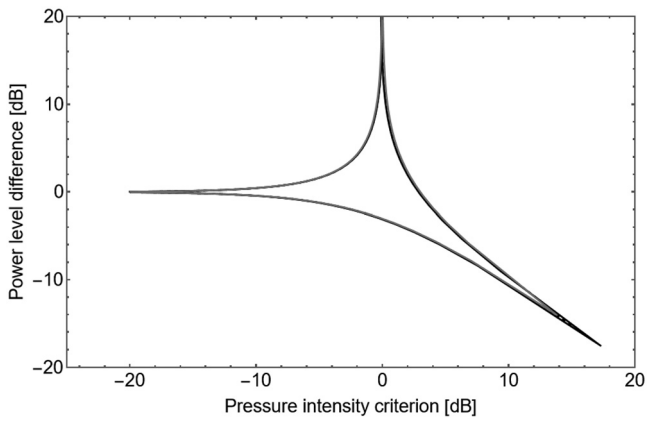

FIG. 2. Power level difference ΔL_W as a function of the pressure intensity criterion $F_{pI\mathrm{n}} - \delta_{pI0}$ for $b_\mathrm{r}/a_\mathrm{r} = 0.1$ (black), $b_\mathrm{r}/a_\mathrm{r} = 1$ (black, dashed), and $b_\mathrm{r}/a_\mathrm{r} = 10$ (gray). All three curves are identical and are plotted in one graph to illustrate this.

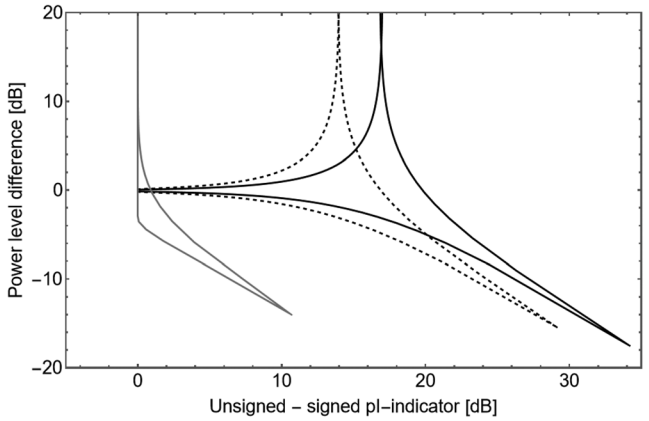

FIG. 3. Power level difference ΔL_W as a function of $F_{p|In|} - F_{pIn}$ for $b_r/a_r = 0.1$ (black), $b_r/a_r = 1$ (black, dashed), and $b_r/a_r = 10$ (gray).

determinations with less than one measurement point are not possible. For the predominantly diffuse extraneous field, relatively small numbers of points are sufficient, whereas for the dominant plane extraneous wave, much larger point numbers are calculated from Eq. (12). This result clearly demonstrates the physical meaning of the SWL difference, which is the difference between the measured SWL and the true SWL. This SWL difference is a systematic error or bias that cannot be reduced by using more measurement points on the enveloping surface. As for Fig. 3, it is, thus, questionable whether the application of the criterion (12) is appropriate to limit the SWL difference.

3. Calculation results for a smaller number of measurement points

The result from the previous clause is that the SWL difference is a clear function of $F_{pIn} - \delta_{pI0}$, whereas the SWL difference depends on the nature of the extraneous sound field for $F_{p|In|} - F_{pIn}$ and N_{min}. However, these three criteria are not alternatively used but additionally in ISO 9614-1,[10] i.e., the result has to be qualified according to all three criteria. To simulate this situation and to use a more reasonable number of measurement points, a spherical array of 12 points with equal point density is used for further calculation. It covers a full sphere. Discrete measurement points are located at the center points of the surfaces of a circumferential regular dodecahedron. Altogether, 1000 random representations with equal distributions are chosen, where δ_{pI0} is between 10 and 25 dB and the relative amplitudes a_r and b_r are between 0 and 5. Additionally, the orientation of the spherical array is randomly chosen. The result is then treated like a measurement result according to ISO 9614-1.[10] All calculated data points lie exactly on the curve defined by Eq. (5). These results are then classified according to criterion (8). The current thresholds of 10 and 7 dB are effectively limiting the SWL deviation to below ±0.5 or ±1.0 dB (Fig. 5). Calculation results that do not fulfill criterion (8) are disqualified and not shown in Fig. 5.

According to ISO 9614-1,[10] results have to additionally comply with criterion (9). For the set of calculation results complying with criterion (8), this test is shown in Fig. 6. There is no correlation at all of the SWL difference with $F_{p|In|} - F_{pIn}$. Disqualifying all results that do not comply with criterion (9) is, therefore, totally unnecessary.

A similar result is obtained for criterion (12). In the considered case, 12 points are used. The calculation of the indicator F_S in combination with the assumption of a survey method ($C = 8$) leads to a disqualification of a large amount of results although their SWL deviation is well within the desired limits (Fig. 7).

C. Dipole

1. Theoretical model

Monopoles are omnidirectional sources. To extend the investigation toward more realistic sources, i.e., sources with a stronger directionality, the monopole from the above model is replaced by a dipole with dipole moment D. The sound pressure at microphones A and B is then

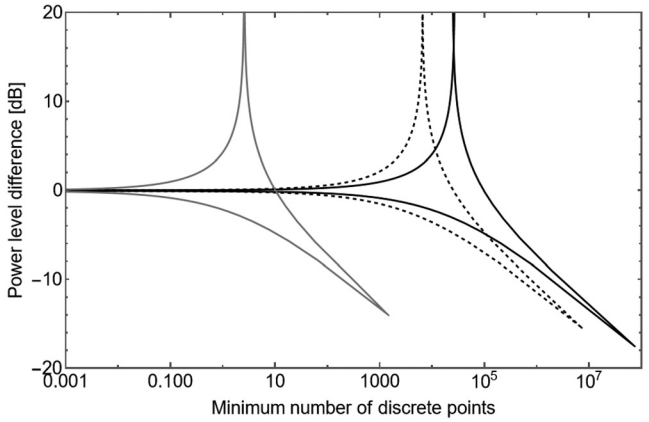

FIG. 4. Power level difference ΔL_W as a function of the minimum number of measurement points [N_{min} from Eq. (12) with $C = 8$] for $b_r/a_r = 0.1$ (black), $b_r/a_r = 1$ (black, dashed), and $b_r/a_r = 10$ (gray).

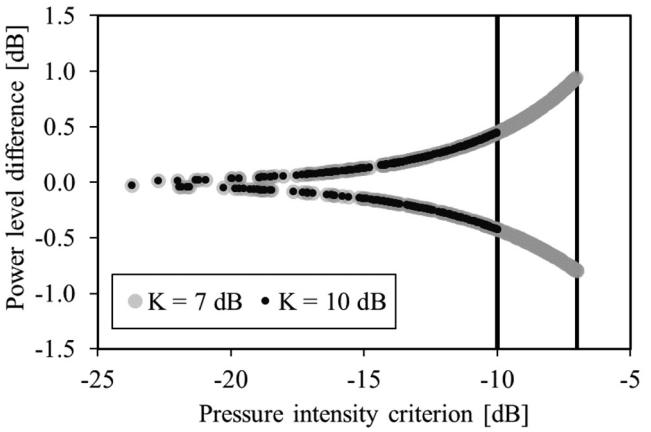

FIG. 5. Power level difference ΔL_W as a function of $F_{pIn} - \delta_{pI0}$ and threshold.

https://doi.org/10.1121/10.0024361

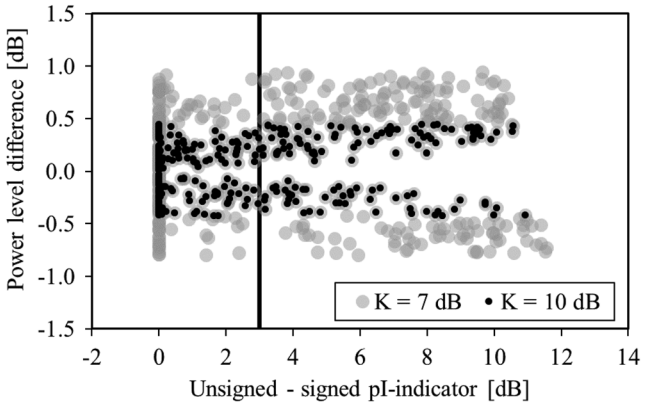

FIG. 6. Power level difference ΔL_W as a function of $F_{p|In|} - F_{pIn}$ and threshold.

$$p_{A/B} = -\frac{\rho\, c\, k^2\, D\, e^{-j\,k\,(r\mp\Delta r)}}{4\,\pi\,(r\mp\Delta r)}\left[1+\frac{1}{j\,k\,(r\mp\Delta r)}\right]\cos\theta + a\, e^{-j\,k\,(r\mp\Delta r)\cos\varphi\sin\theta} + b. \tag{21}$$

Introducing this expression into Eq. (13) gives the intensity related to the area of the enveloping surface S and the sound power of the dipole [see also Eq. (16)],

$$I_r = \frac{3\cos^2\theta}{k\,2\,\Delta r}\frac{1}{\left[1-(\Delta r/r)^2\right]}\sqrt{1+\left[\frac{1}{k\,r\,(1-\Delta r/r)}\right]^2} \times\sqrt{1+\left[\frac{1}{k\,r\,(1+\Delta r/r)}\right]^2} \times\sin\left(k\,2\,\Delta r-\arctan\left[\frac{1}{k\,r\,(1-\Delta r/r)}\right] +\arctan\left[\frac{1}{k\,r\,(1+\Delta r/r)}\right]\right) + 3\,a_r^2\,\frac{\sin(k\,2\,\Delta r\cos\varphi\sin\theta)}{k\,2\,\Delta r} + \mathrm{sgn}(\Delta\phi)\,p_r^2\,10^{-0.1\,\delta_{pI0}/\mathrm{dB}} \tag{22}$$

with the related sound pressure

$$p_r = \sqrt{\frac{3}{4}}\left\{\sqrt{\left[\frac{\cos\theta}{(1-\Delta r/r)}\right]^2\left\{1+\left[\frac{1}{k\,r\,(1-\Delta r/r)}\right]^2\right\}+a_r^2+b_r^2}+\sqrt{\left[\frac{\cos\theta}{(1+\Delta r/r)}\right]^2\left\{1+\left[\frac{1}{k\,r\,(1+\Delta r/r)}\right]^2\right\}+a_r^2+b_r^2}\right\} \tag{23}$$

and the related amplitudes of the plane wave a_r and the diffuse field b_r,

$$a_r = a\,\frac{4\,\pi\,r}{\rho\,c\,k^2\,D};\quad b_r = b\,\frac{4\,\pi\,r}{\rho\,c\,k^2\,D}. \tag{24}$$

As for the monopole case, a correlation between the direct field from the dipole, the diffuse field, and the plane wave is suppressed in the derivation of Eq. (22).

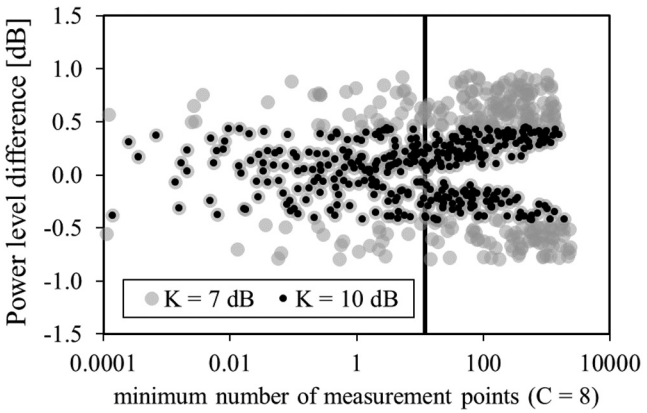

FIG. 7. Power level difference ΔL_W as a function of N_{min} for a monopole and threshold.

2. Calculation results

For infinitely large numbers of measurement points, calculation results are qualitatively identical to the monopole case. For the sake of brevity, they are therefore not presented here.

Then the 12-point array described in Sec. III B 3 was used. Again, 1000 random calculations were performed with random lateral orientation of the array and equal distributions of δ_{pI0} between 10 and 25 dB and a_r and b_r between 0 and 2. The upper limits of the relative sound pressure amplitudes are smaller than for the presented monopole results, because they are related to the sound pressure of the dipole in its maximum direction [Eq. (24)].

The calculation results for the power level difference ΔL_W as a function of $F_{pIn} - \delta_{pI0}$ and $F_{p|In|} - F_{pIn}$ are identical to Figs. 5 and 6. Therefore, they are not shown again. A clear difference from the monopole case is observed for the power level difference ΔL_W as a function of N_{min} (Fig. 8). The indicator F_S is much larger than for the monopole case since the spatial variation of the sound field is much larger. Therefore, a larger number of measurement points is required according to Eq. (12) for the dipole (Fig. 8) compared to the monopole (Fig. 7). Still, to limit the SWL deviation, an application of criterion (8) is absolutely sufficient,

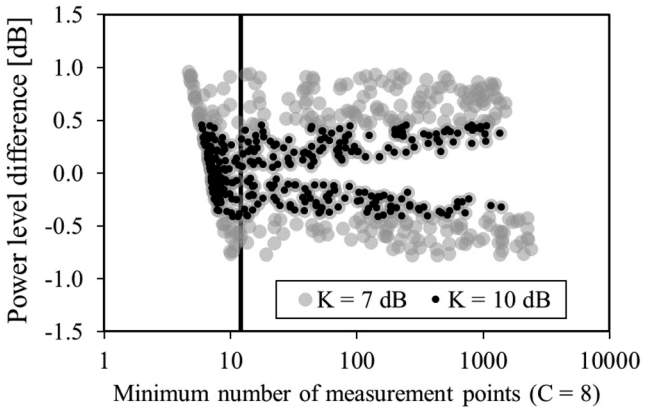

FIG. 8. Power level difference ΔL_W as a function of $N_{\min}$ for a dipole and threshold.

whereas criterion (12) unnecessarily disqualifies correct measurement results.

IV. EXPERIMENTAL VERIFICATION

A. Sources and surrounding environments

A major aim of the contribution was to perform measurements to verify the theoretical findings. Two main topics stand out from the theoretical calculations. The first is the utility of the $F_{pI\mathrm{n}} - F_{p|I\mathrm{n}|}$ criterion, and the second is the minimum number of the required measurement points $N_{\min}$. The difference between the pressure intensity indices is related to the presence of extraneous noise and/or strong reverberation, whereas the number of points is related to the field non-uniformity.[10–12] The measurements were structured to cover a wide range of sources, environments, background noise characteristics, and other influential parameters, and apparently, it is assumed they can be used for supporting the ISO 9614[10–12] revision proposals.

Four sources were used, varying in spectral content (broad- and narrowband), directivity, and absorption. Figure 9 shows all sources, namely, a BS, BSWA, a TS, and a TSWA. As can be seen, BS is an assembly of two aerodynamic reference sound sources [type 4204; Brüel & Kjaer (Naerum, Denmark)] positioned at different heights provided by a wooden box, having one side open. TS is a half-dodecahedron loudspeaker, which emits a multi-sine signal following

$$s = A \sum_{i=1}^{31} \sin(2\pi f_i + \varphi_i), \tag{25}$$

where A is the amplitude, f_i the center frequency of the ith one-third octave band from 20 Hz to 20 kHz rounded to the nearest decade, and φ_i the related phase. The latter was

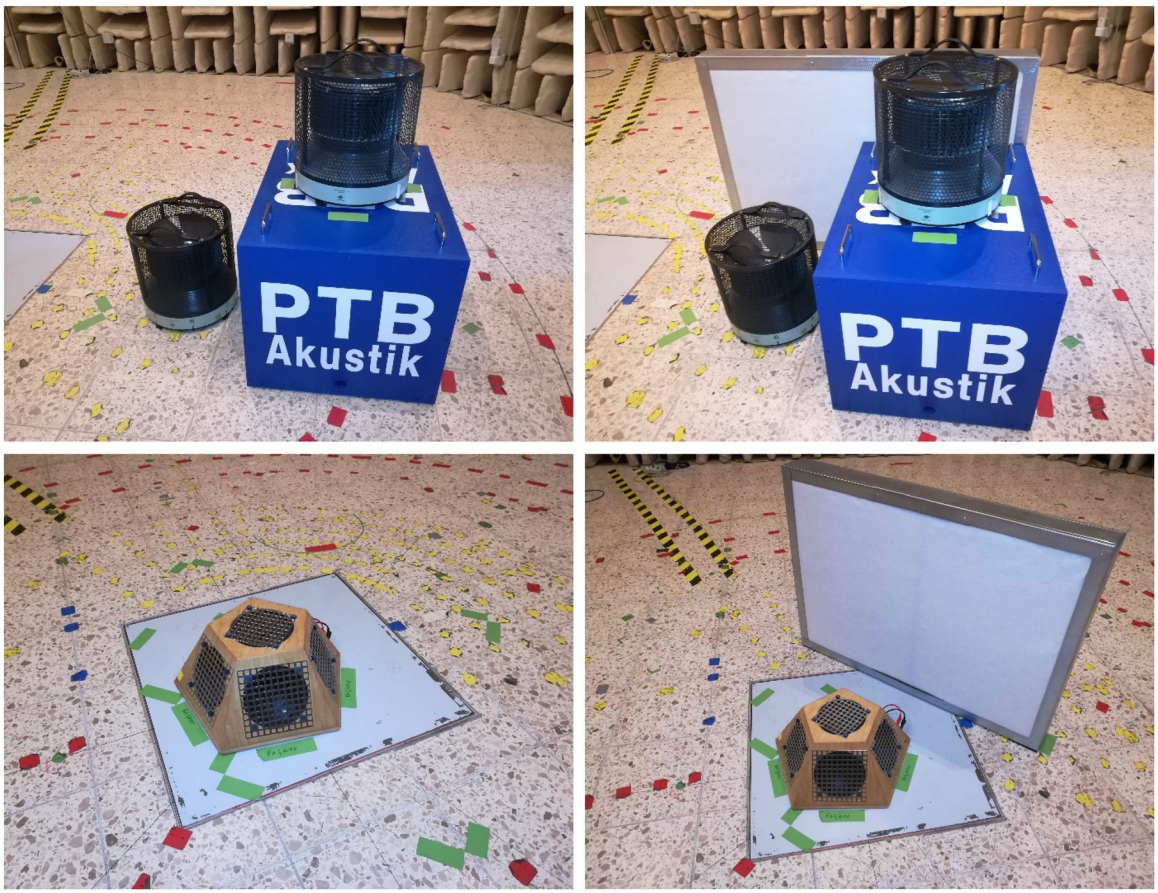

FIG. 9. (Color online) Sources under test: broadband source (BS) (top left), broadband source with absorption (BSWA) (top right), tonal source (TS) (bottom left), and tonal source with absorption (TSWA) (bottom right).

https://doi.org/10.1121/10.0024361

randomly generated for each discrete frequency once. Then it was used for all TS measurements for repeatability reasons. To account for any changes in the sound emission of the TS, a correction was applied. It is given by

$$C_{\mathrm{em}} = 10\,\mathrm{lg}\left(\frac{\mathrm{Re}\{S_{V_{\mathrm{in}}I_{\mathrm{in}}}\}}{\mathrm{Re}\{S_{V_{\mathrm{in}}I_{\mathrm{in,\,ref}}}\}}\right)\mathrm{dB}, \tag{26}$$

where $\mathrm{Re}\{S_{V_{\mathrm{in}}I_{\mathrm{in}}}\}$ is the real part of the cross-spectrum of the input voltage and current of the signal fed to the TS, and $\mathrm{Re}\{S_{V_{\mathrm{in}}I_{\mathrm{in,\,ref}}}\}$ is a reference cross-spectrum. The latter was set as the mean value of all cross-spectra used. Minor changes in the acoustic emission of the TS were revealed after the application of the correction. The signal correction was also applied to TSWA.

BSWA and TSWA are modifications of BS and TS, respectively. For the modification, an absorbing panel was added to each source at a defined position. For BSWA, the panel covered the open side of the box. The absorber had a thickness of 100 mm and a surface of 0.7 m^2. It was made of a polyester fiber mat, which is framed by a U-shaped aluminum profile.

Measurements were performed in five rooms, Physikalisch-Technische Bundesanstalt (PTB)'s hemi-anechoic room, PTB's 200 m^3 reverberation room, an open space (a basement), a 50 m^3 reverberant room, and the same room after adding absorption. For variation purposes, the hemi-anechoic room was used in two different states. In the first, the room was used as normal, while in the second, reflections were added. This was realized by adding ten reflecting panels of 0.7 m^2 each. They were placed in front of the wedges on two orthogonal sides of the room, five on each side.

B. Probe positioning

Following the guidelines of the ISO 9614[10–12] series, measurements were performed either by scanning or at discrete points. The movement or positioning of the probes was performed both by automated means and manually. Three sound intensity probes were used, accommodating Brüel & Kjaer phase-matched microphone pairs.[18] Three pairs of type 4181 and one of type 4197 were available for selection. For each measurement, two pairs of type 4181 and type 4197 were connected to the intensity probes.

1. Automated measurements

The automated measurements were performed in PTB's hemi-anechoic room using PTB's scanning apparatus,[19] covering a hemispherical measurement surface of 1.7 m radius. The scanning apparatus was placed inside PTB's hemi-anechoic room, which is qualified according to ISO 26101-1[20] for frequencies between 50 Hz and 20 kHz for the measurement radii used. For the full scan of the hemisphere, the three probes covered once the left quarter sphere and afterward the right quarter sphere. For the measurements at discrete points, the arc movement was remotely stopped at predefined positions, occurring at 15°, 45°, 75°, 105°, 135°, and 165° (angle between the floor and the arc). This provided 36 measurement points.

A preliminary investigation was about the influence of the scanning speed. It must be noted that the speed of each probe is different due to its position on the scanning apparatus. Measurements were performed for three different measurement durations, namely, $T = 600$ s, $T = 900$ s, and $T = 1200$ s, revealing no significant differences among the results. The scan duration is related to the temporal stability of the random signal of BS and BSWA, and according to a previous analysis,[21] the measurement duration for the automated scanning measurements was set to 1200 s. For the automated measurements at discrete points, the measurement duration was 180 s for each point.

2. Manual measurements

The manual measurements were performed by both scanning and measurements at discrete points. A specially assembled holder, which could be screwed onto a microphone stand, allowed the simultaneous use of all three probes. The holder can be seen in Fig. 10. This allowed the variation of the surface sampling by using all three probes or only the middle one. The separation between the probes on the holder was 0.24 m.

Contrary to the use of a hemisphere in the automated measurements, the manual measurements were performed over a parallelepiped of varying surface due to the different environmental surroundings.

During the manual measurements, special effort was made to keep the scanning speed lower than 0.5 m/s and as constant as possible, according to the ISO 9614[11,12] requirements. For the measurements at discrete points, each partial surface was divided into 0.5 m × 0.5 m squares. Using all three probes led to 128 measurement points for the measurements in the hemi-anechoic room, the open space, and the reverberant room and to 78 points for the measurements in the reverberation room. For single probe measurements, the

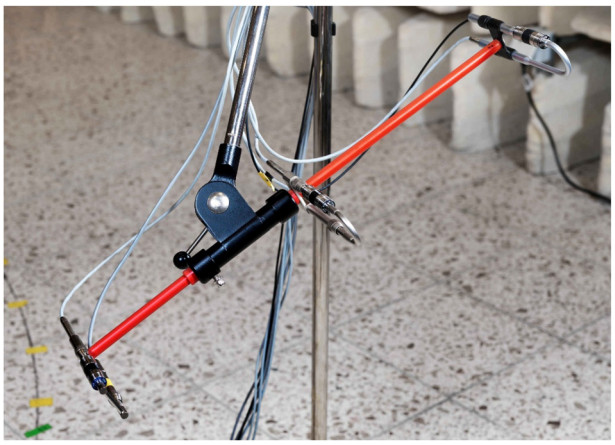

FIG. 10. (Color online) Holder to accommodate three sound intensity probes on a microphone stand for the manual measurements.

point number is 64 and 26, respectively. Sound intensity was measured for 60 s at each point.

C. Measured quantities

1. Sound intensity and sound pressure

The sound pressure signals were recorded by a multi-channel analyzer, which calculated the auto-spectra and the complex cross-spectra in real time, using a fast Fourier transform (FFT) algorithm with 6401 lines and applying a Hanning window. The spectra were appropriately averaged by the analyzer, depending on the measurement duration, and they were further processed using MATLAB.

The sound intensity was calculated from the cross-spectrum of each microphone pair according to

$$I(\omega) = \frac{1}{\omega\,\rho\,2\,\Delta r}\,\mathrm{Im}\{S_{p_1p_2}(\omega)\}, \tag{27}$$

where ω is the angular frequency, ρ the air density, Δr the spacer length, and $\mathrm{Im}\{S_{p_1p_2}(\omega)\}$ the imaginary part of the microphone pair cross-spectrum.[22] The spacer length was determined by the finite difference error,[23] which is given by

$$\Delta L_I = 10\,\lg\left[\frac{\sin(k\,2\,\Delta r)}{k\,2\,\Delta r}\right]\mathrm{dB}. \tag{28}$$

For the measurements at lower frequencies, a 50 mm spacer was used up to the frequency determined by Eq. (28) as the point where ΔL_I exceeds 0.5 dB. For the higher frequency measurements, a 12 mm spacer was used.[24]

The one-third octave bands from 50 Hz to 10 kHz were calculated from FFT bands by adding all M intensity FFT lines ω_m belonging to the corresponding one-third octave band as

$$I = \sum_{m=1}^{M} I(\omega_m). \tag{29}$$

In relation to the finite difference error, for the bands up to 800 Hz, the 50 mm spacer was used, whereas for the higher frequencies, the 12 mm spacer was used.

For the sound pressure, this summation was performed energetically by

$$p^2 = \sum_{m=1}^{M}\left[\frac{p^2_{\mathrm{A}(\omega_m)} + p^2_{\mathrm{B}(\omega_m)}}{2}\right], \tag{30}$$

where p_{A} and p_{B} are the sound pressure signals of each microphone.

Due to the frequency characteristics of the TS and the TSWA input signals, an alternative calculation of the one-third octave bands was applied. In this, only the lines corresponding to the one-third octave band center frequencies and their directly adjacent lines were used (in total three FFT lines for each one-third octave band). The adjacent lines were considered due to the side lobes of the Hanning window applied to the FFT analysis.

2. Pressure-residual intensity index

The pressure-residual intensity index is defined as the difference between the indicated sound pressure level $L_{p,\Delta p=0}$ and sound intensity level of the residual intensity $L_{I,\mathrm{res}}$, when the intensity probe is placed and oriented in a sound field whose sound intensity is zero,[12] using a specially designed coupler. The index is calculated from Eq. (3).

The level of the residual intensity I_{res} is given by

$$L_{I,\mathrm{res}} = 10\,\lg\frac{|I_{\mathrm{res}}|}{I_0}\,\mathrm{dB}. \tag{31}$$

The pressure-residual intensity index depends on the spacer length. The relation between the spacer lengths used in the study is

$$\begin{aligned}\delta_{pI0(50\,\mathrm{mm})} &= \delta_{pI0(12\,\mathrm{mm})} + 10\,\lg\frac{50}{12}\,\mathrm{dB}\\ &\approx \delta_{pI0(12\,\mathrm{mm})} + 6.2\,\mathrm{dB}.\end{aligned} \tag{32}$$

For the residual intensity measurements, the Brüel & Kjaer ZI 0055 sound source was used. The generated signal is emitted up to 5 kHz, which is the cut-off frequency of the built-in filter. The source was also externally driven, but it was not possible for frequencies above 5 kHz to emit. Due to the application of the sound intensity measurements to frequencies above 5 kHz, this value was used for higher frequencies. The pressure-residual intensity index is given in Fig. 11. As may be seen, the connection line appears to be sensitive to many parameters, e.g., the microphone preamplifier. For this reason, the pressure-residual intensity index was measured each time there were changes in the connection line.

D. Extraneous noise

In the current state-of-the-art procedures, actions are proposed in case extraneous noise disturbs the sound intensity measurements.[10–12] To investigate the influence of extraneous noise, a set of measurements was performed in the hemi-anechoic room. A loudspeaker used for facade measurements was utilized as a source of extraneous noise. It was positioned at a corner of the hemi-anechoic room so that it radiated through the measurement surface. The loudspeaker was fed with white noise by a noise generator. Measurements were performed at various noise levels compared to the time and surface-averaged sound pressure level of the source. Measurements were performed with and without noise. For the former, the difference between the level of the source under test and the overall noise level was –10, –5, 0, 5, and 10 dB. The level difference was individually set for each source under test through a graphic equalizer.

An important characteristic of extraneous noise is its stationarity. The measurements included both stationary and non-stationary extraneous noise. The stationary noise measurements were performed while the facade loudspeaker was uninterruptedly emitting during the entire measurement. The non-stationary noise measurements were performed by

https://doi.org/10.1121/10.0024361

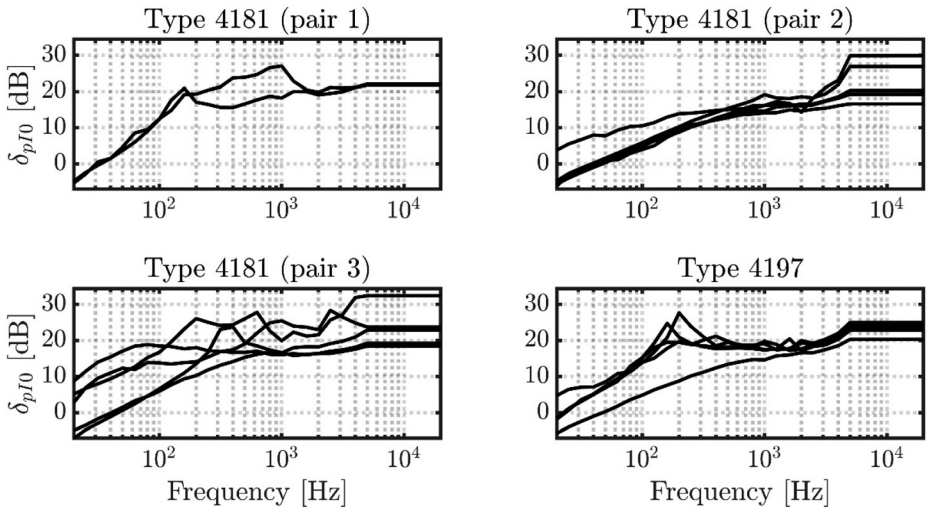

FIG. 11. Pressure-residual intensity index for all microphone pairs. Each line corresponds to a different date and connection line. The index corresponds to a 12 mm spacer.

different configurations depending on the measurement method. For the automated scanning, the measurements were divided into four equal time intervals, and the noise emission was successively switched, e.g., noise—no noise—noise—no noise. For the automated measurements at discrete points, the combination of measurements at different noise levels allowed the non-stationarity of the noise. For half of the points, the measurements without noise were considered, while for the other half, measurements with noise were considered. The same approach was also used for the manual measurements. For the partial surfaces parallel to the facade loudspeaker axis, the measurements without noise were used, while for the partial surfaces perpendicular to the axis, the measurements with noise were used.

The measurements performed concerning the influence of the extraneous noise are summarized in Table I, and those concerning the influence of the surrounding environment are shown in Table II (see Appendix).

E. Utility of the indicator $F_{p|I_n|}$

The unsigned pressure intensity indicator is used to check the presence of strong extraneous noise in comparison to the signed pressure intensity indicator.[10,12] In the theoretical investigation, it was shown that the deviation of the SWL from the actual level is not correlated to this criterion. This was also the case for the measurement results described in Tables I and II (see Appendix). The measurement results were used as follows. The SWLs of all sources for measurements during strong extraneous noise ($\overline{L_p} - L_n = 0, -5$, and -10 dB) were considered. The deviation from the SWL determined after automated scanning measurements without extraneous noise was set as the related SWL difference using

$$\Delta L_{W(\text{noise})} = L_{W(\text{noise})} - L_{W(\text{scan, no noise})}. \tag{33}$$

The SWL differences were checked according to the $F_{pIn} - \delta_{pI0}$ criterion and are presented in Fig. 12 for both values of the bias error factor K. It must be noted that for the SWL determination using a single probe, the corresponding δ_{pI0} was used, while for the case of three probes, the lowest value of the three δ_{pI0} was selected for each frequency. The graph reveals no correlation between the two quantities and is, thus, an experimental support to the theoretical findings regarding the redundancy of the unsigned pressure intensity indicator.

F. Investigation on the required number of measurement points

An analysis was performed to check the correlation between the non-homogeneity indicator F_S and the number of measurement points based on the discrete point measurements as follows. The indicator was estimated using Eq. (1), and following the theoretical calculation, the number of minimum points was then calculated using Eq. (12). The value of the factor C was 8, which corresponds to survey grade results.[10] As previously, the SWL difference was calculated by setting the SWL determined after automated scanning measurements as reference, using

$$\Delta L_{W(\text{points})} = L_{W(\text{discrete})} - L_{W(\text{scan, no noise})}. \tag{34}$$

As stated in Sec. IV E, the qualification of the results was performed using the $F_{pIn} - \delta_{pI0}$ criterion of Eq. (8). The SWL difference is shown against the number of minimum points $N_{\min}$ in Fig. 13. Again, a correlation between the

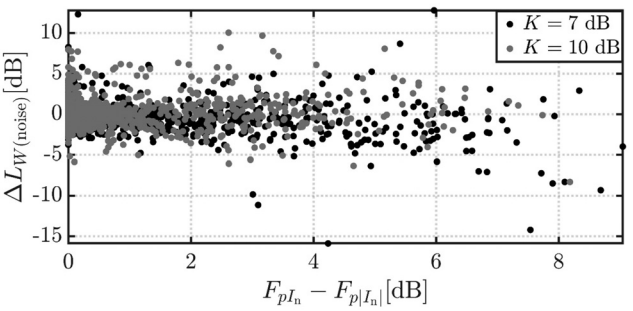

FIG. 12. SWL deviation from the reference level against the difference between the signed and unsigned pressure intensity indicator.

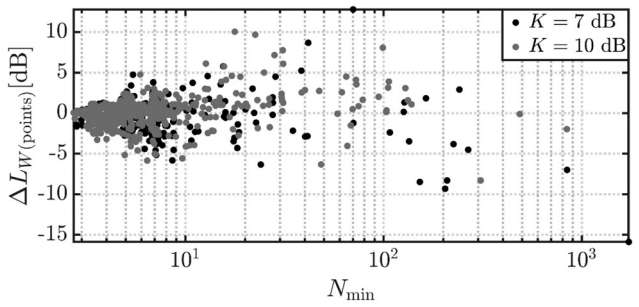

FIG. 13. SWL deviation from the reference level against the minimum number of measurement points.

SWL difference and the number of the required measurement points is not supported.

V. CONCLUSION

This paper investigates the use of field indicators for standardized measurements with a p-p sound intensity probe that aim to determine the SWL of a source. In the current ISO 9614 set of standards,[10–12] the field indicators are used to define criteria to assess the quality of the measured SWL and to decide whether or not a valid result has been obtained. To test the validity of these criteria, analytic calculations of the SWL measured by a p-p sound intensity probe for sources of different order (monopole and dipole), in part superposed by extraneous noise in the form of a plane wave and a diffuse sound field, were performed. These calculations delivered new insights regarding the correlation of the currently used field indicators with the deviation of the measured SWL from the actual SWL.

These theoretical results were confirmed by the results of the experiments, described in Sec. IV. Thus, we conclude that the unsigned pressure intensity indicator $F_{p|In|}$ and the non-homogeneity indicator F_S do not provide any useful information regarding the quality of the measured SWL. We propose to assess the quality of the measured SWLs using solely the signed pressure intensity index F_{pIn} in combination with the pressure-residual intensity index δ_{pI0}. The present research can be the basis for further investigation, which could be used as guidance in a future revision of the whole ISO 9614 set of standards.

A revised and, thus, simplified ISO 9614 set of standards would help machinery manufacturers and other users by reducing the measurement effort for the sound power determination. This, in turn, will improve the reliability of noise emission data of machines and ensure fair competition toward quieter machines. Reliable noise emission data are necessary for employers and users of machines to preferably sell and buy quieter machines (Sell and Buy Quiet). With reliable data, employers can more strategically replace noisy equipment with quieter equipment. Replacing noisy equipment with quieter equipment is one way to better protect their workers from noise.

ACKNOWLEDGMENTS

Presented results were obtained within a research project undertaken at PTB and funded by the Federal Institute for Occupational Safety and Health (BAuA) as a subproject (F2450) of a focus project aiming at the simplification of noise emission measurement methods. The authors thank Heinrich Bietz for performing measurements at PTB's reverberation room and Kevin Picker for performing a considerable number of the intensity measurements.

AUTHOR DECLARATION

Conflict of Interest

The authors have no conflicts to disclose.

DATA AVAILABILITY

The data that support the findings of this study are available from the corresponding author upon reasonable request.

APPENDIX

A descriptive list of the measurement sets that were performed during the research project is presented. The list is displayed in Tables I and II for better clarity.

TABLE I. List of measurements for the influence of extraneous noise.

Source	Environment	Measurement surface	Sampling	$\overline{L_p} - L_n$	Noise type
BS TS BSWA TSWA	Hemi-anechoic room	Hemisphere	Scan, discrete points (automated)	$\overline{L_p}$, −10 dB, −5 dB, 0 dB, 5 dB, 10 dB	Stationary, non-stationary
BSWA TSWA	Hemi-anechoic room + reflection				
BS TS BSWA TSWA	Hemi-anechoic room	Parallelepiped	Scan, discrete points (manual)	$\overline{L_p}$, 0 dB, 5 dB, 10 dB	

https://doi.org/10.1121/10.0024361

TABLE II. List of measurements for the influence of the surrounding environment.

Source	Environment	Measurement surface	Sampling	$\overline{L_p} - L_n$	Noise type
BS TS BSWA TSWA	(a) Reverberation room, (b) open space, (c) reverberant room, (d) reverberant room + absorption	Parallelepiped	Scan, discrete points (manual)	$\overline{L_p}$	

[1]European Parliament and European Council, "Directive 2000/14/EC of the European Parliament and of the Council of 8 May 2000 on the approximation of the laws of the Member States relating to the noise emission in the environment by equipment for use outdoors," OJEC **L 162**, 1–78 (2000).

[2]Government of Western Australia, "Noise Abatement (Noise Labelling of Equipment) Regulations (No. 2) 1985," in *Environmental Protection Act 1986* (Government of Western Australia, Perth, Australia, 1985), pp. 2549–2551.

[3]State of New South Wales and Environment Protection Authority, *The Protection of the Environment Operations (Noise Control) Regulation 2017—Approved Methods for Testing Noise Emissions* (Environmental Protection Authority, Sydney, Australia, 2017).

[4]European Parliament and European Council, "Directive 2006/42/EC of the European Parliament and of the Council of 17 May 2006 on machinery, and amending Directive 95/16/EC (recast)," OJEU **L 157**, 24–86 (2006).

[5]European Parliament and European Council, "Directive 2009/125/EC of the European Parliament and of the Council of 21 October 2009 establishing a framework for the setting of ecodesign requirements for energy-related products," OJEU **L 285**, 10–35 (2009).

[6]European Commission, "Commission Delegated Regulation (EU) 2019/2017 of 11 March 2019 supplementing Regulation (EU) 2017/1369 of the European Parliament and of the Council with regard to energy labelling of household dishwashers and repealing Commission Delegated Regulation (EU) No. 1059/2010," OJEU **L 315**, 134–154 (2019).

[7]A. M. Ondet and L. J. Barbry, "Modeling of sound propagation in fitted workshops using ray tracing," J. Acoust. Soc. Am. **85**(2), 787–796 (1989).

[8]M. Hodgson, "Ray-tracing evaluation of empirical models for predicting noise in industrial workshops," Appl. Acoust. **64**(11), 1033–1048 (2003).

[9]ISO 3740:2019, "Acoustics—Determination of sound power levels of noise sources—Guidelines for the use of basic standards" (International Organization for Standardization, Geneva, Switzerland, 2019).

[10]ISO 9614-1:1993, "Acoustics—Determination of sound power levels of noise sources using sound intensity—Part 1: Measurement at discrete points" (International Organization for Standardization, Geneva, Switzerland, 1993).

[11]ISO 9614-2:1996, "Acoustics—Determination of sound power levels of noise sources using sound intensity—Part 2: Measurement by scanning" (International Organization for Standardization, Geneva, Switzerland, 1996).

[12]ISO 9614-3:2002, "Acoustics—Determination of sound power levels of noise sources using sound intensity—Part 3: Precision method for measurement by scanning" (International Organization for Standardization, Geneva, Switzerland, 2002).

[13]ISO 3744:2010, "Acoustics—Determination of sound power levels and sound energy levels of noise sources using sound pressure—Engineering methods for an essentially free field over a reflecting plane" (International Organization for Standardization, Geneva, Switzerland, 2010).

[14]F. Jacobsen, "Sound field indicators: Useful tools," Noise Control Eng. J. **35**(1), 37–46 (1990).

[15]F. Jacobsen, "Sound intensity measurements," in *Handbook of Noise and Vibration Control*, edited by M. J. Crocker (Wiley, New York, 2007), pp. 534–548.

[16]F. Jacobsen, "A simple and effective correction for phase mis-match in intensity probes," Appl. Acoust. **33**, 165–180 (1991).

[17]G. Hübner, "The use of sound field indicators for the measurement of the sound intensity determined sound power," in *Proceedings of INTER-NOISE 89*, Newport Beach, CA (December 4–6, 1989) (Institute of Noise Control Engineering, Washington, DC), pp. 1015–1020.

[18]IEC 61043:1993, "Electroacoustics—Instruments for the measurement of sound intensity—Measurements with pairs of pressure sensing microphones" (International Electrotechnical Commission, Geneva, Switzerland, 1993).

[19]S. Brezas, C. Bethke, and V. Wittstock, "A new scanning apparatus for the dissemination of the unit Watt in airborne sound," in *Proceedings of DAGA 2016*, Aachen, Germany (March 14–17, 2016) [German Acoustical Society (DEGA), Berlin, Germany], pp. 1270–1273.

[20]ISO 26101-1: 2021, "Test methods for the qualification of the acoustic environment—Part 1: Qualification of free-field environments" (International Organization for Standardization, Geneva, Switzerland, 2021).

[21]S. Brezas and V. Wittstock, "Study on the properties of aerodynamic reference sound sources," Acta Acust. united Acust. **105**, 960–969 (2019).

[22]W. W. Lang, G. C. Maling, M. A. Nobile, Jr., and J. Tichy, "Determination of sound power levels and directivity of noise sources," in *Noise and Vibration Control Engineering*, edited by I. L. Vér and L. L. Beranek (Wiley, New York, 2006), p. 104.

[23]F. Jacobsen, "On the uncertainty in measurement of sound power using sound intensity," Noise Control Eng. J. **55**, 20–28 (2007).

[24]F. Jacobsen, V. Cutanda, and P. M. Juhl, "A numerical and experimental investigation of the performance of sound intensity probes at high frequencies," J. Acoust. Soc. Am. **103**, 953–961 (1998).